Synthesis, Structure, and Redox and Catalytic Properties of a New Family of Ruthenium Complexes Containing the Tridentate bpea Ligand

Montserrat Rodríguez, Isabel Romero, and Antoni Llobet*

Departament de Química, Universitat de Girona, Campus de Montilivi, E-17071 Girona, Spain

Alain Deronzier

Laboratoire d'Electrochimie Organique et Photochimie Rédox (URA CNRS D1210), Université Joseph Fourier Grenoble 1, BP 53X, 38041 Grenoble Cedex, France

Margret Biner

Departement für Chemie und Biochemie, Universität Bern, CH-3000 Bern 9, Switzerland

Teodor Parella

Departament de Química, Universitat Autònoma de Barcelona, Bellaterra, E-08193 Barcelona, Spain

Helen Stoeckli-Evans

Institute of Chemistry, University of Neuchatel, Av. Bellevaux 51, CH-2000 Neuchatel, Switzerland

Received January 17, 2001

We have prepared a new family of ruthenium complexes containing the bpea ligand (where bpea stands for *N*,*N*-bis(2-pyridyl)ethylamine), with general formula $[Ru(bpea)(bpy)(X)]^{n+}$ (**2**, X = Cl^-; **3**, X = H_2O; **4**, X = OH^-), and the trisaqua complex $[Ru(bpea)(H_2O)_3]^{2+}$, **6**. The complexes have been characterized through elemental analyses, UV−vis and ^1H NMR spectroscopy, and electrochemical studies. For complex **3**, the X-ray diffraction structure has also been solved. The compound belongs to the monoclinic $P2_1/m$ space group, with $Z = 2$, $a = 7.9298(6)$ Å, $b = 18.0226(19)$ Å, $c = 10.6911(8)$ Å, and $\beta = 107.549(8)°$. The Ru metal center has a distorted octahedral geometry, with the O atom of the aquo ligand placed in a trans position with regard to the aliphatic N atom of the bpea ligand so that the molecule possesses a symmetry plane. NMR spectra show that the complex maintains its structure in aqueous solution, and that the corresponding chloro complex also has a similar structural arrangement. The pH dependence of the redox potential for the complex $[Ru(bpea)(bpy)(H_2O)](PF_6)_2$ is reported, as well as the ability of the corresponding oxo complex to catalyze the oxidation of benzylic alcohol to benzaldehyde in both chemical and electrochemical manners.

Introduction

A family of $Ru^{II}-OH_2$ complexes bearing different ligands has been extensively described that by sequential proton and electron loss are capable of reaching higher oxidation states within a relatively narrow potential range.[1] The following equations illustrate those processes for the $[Ru^{II}(trpy)(bpy)(H_2O)]^{2+}$ complex:[1a]

$$[Ru^{II}(trpy)(bpy)(H_2O)]^{2+} \underset{+1H^+,\,+1e^-}{\overset{-1H^+,\,-1e^-}{\rightleftharpoons}} [Ru^{III}(trpy)(bpy)(OH)]^{2+} \quad (1)$$

$$E_{1/2}(Ru^{III/II} \text{ at pH } 7) = 0.49 \text{ V vs SSCE}$$

$$[Ru^{III}(trpy)(bpy)(OH)]^{2+} \underset{+1H^+,\,+1e^-}{\overset{-1H^+,\,-1e^-}{\rightleftharpoons}} [Ru^{IV}(trpy)(bpy)(O)]^{2+} \quad (2)$$

$$E_{1/2}\,(Ru^{IV/III} \text{ at pH } 7) = 0.62 \text{ V vs SSCE}$$

Those complexes are of interest because their higher oxidation states are capable of performing a variety of oxidation reactions in both stoichiometric and catalytic manners. Organic and

* To whom correspondence should be addressed. E-mail: antoni.llobet@udg.es.

(1) (a) Binstead, R. A.; Meyer, T. J. *J. Am. Chem. Soc.* **1987**, *109*, 3287. (b) Sinha, P. K.; Chakravarty, J.; Bhattacharya, S. *Polyhedron* **1996**, *15*, 2931. (c) Sadakne, M.; Steckhan, E. *Chem. Rev.* **1998**, *98*, 219. (d) Kubow, S. A.; Marmion, M. E.; Takeuchi, K. J. *Inorg. Chem.* **1988**, *27*, 2761. (e) Che, C. M.; Lai, T. F.; Wong, K. Y. *Inorg. Chem.* **1987**, *26*, 2289. (f) Moyer, B. A.; Meyer, T. J. *Inorg. Chem.* **1981**, *20*, 436. (g) Ho, C.; Che, C.-M.; Lau, T.-C. *J. Chem. Soc., Dalton Trans* **1991**, 1901. (h) Che, C.-M.; Wong, K. I.; Leung, W. H.; Poon, C. K. *Inorg. Chem.* **1986**, *25*, 345. (i) Marmion, M. E.; Takeuchi, K. J. *J. Am. Chem. Soc.* **1986**, *108*, 510. (j) Muller, J. H.; Acquaye, J. H.; Takeuchi, K. J. *Inorg. Chem.* **1992**, *31*, 4552. (k) Gerli, A.; Reedijk, Lakin, M. T.; Spek, A. L. *Inorg. Chem.* **1995**, *34*, 1836. (l) Hua, X.; Shang, M.; Lappin, A. G. *Inorg. Chem.* **1997**, *36*, 3735.

10.1021/ic010064q CCC: $20.00
Published on Web 07/13/2001

inorganic substrates such as alkanes,[2] alkenes,[3] alcohols,[4] phosphines,[5] and sulfides[6] have been catalytically oxidized using this type of compound.

The redox properties of the $Ru-OH_2$ complexes and their corresponding higher oxidation state species can be controlled by choosing the appropriate ancillary ligands. As an example, the $E_{1/2}$ values of the Ru(III)/Ru(II) couple for $[Ru^{II}(NH_3)_5(H_2O)]^{2+}$ and $[Ru^{II}(trpy)(dppene)(H_2O)]^{2+}$ (dppene is *cis*-1,2-bis(diphenylphosphino)ethylene) differ by 1.50 V at pH 7 under similar conditions.[7] This tremendous difference in redox potentials is due to the different steric[8] and electronic properties that the ligands are capable of transmitting to the metal center via σ and π interactions.

With the aim to further elucidate the different parameters that govern the redox properties and the performance of the Ru=O redox catalysts, we have prepared and characterized a new $Ru-OH_2$ complex containing the tridentate polypyridylic ligand *N*,*N*-bis(2-pyridylmethyl)ethylamine (bpea) and the didentate 2,2′-bipyridine (bpy) ligand.

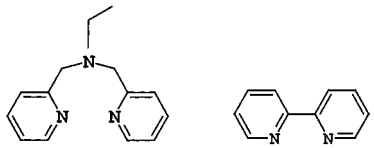

Here we present the synthesis and structural, spectroscopic, and electrochemical characterization of $[Ru^{II}(bpea)(H_2O)_3]^{2+}$ and of complexes of general formula $[Ru^{II}(bpea)(bpy)X]^{n+}$ (X = Cl, H_2O) together with the capacity of its corresponding Ru^{IV}=O complexes to catalytically and electrocatalytically oxidize benzyl alcohol to benzaldehyde.

Experimental Section

Materials. All reagents used in the present work were obtained from Aldrich Chemical Co. and were used without further purification. Reagent grade organic solvents were obtained from SDS, and high purity deionized water was obtained by passing distilled water through a nanopure Milli-Q water purification system. $RuCl_3 \cdot 2H_2O$, **1**, was supplied by Johnson and Matthey Ltd. and was used as received.

Preparations. The bpea ligand and the $[Ru^{II}(H_2O)_6](p\text{-tos})_2 \cdot 1.5H_2O$, **5·1.5H$_2$O** (*p*-tos is the *p*-toluenesulfonate anion), complex were prepared according to literature procedures.[9,10c] All synthetic manipulations were routinely performed under a nitrogen atmosphere using Schlenck tubes and vacuum line techniques. Electrochemical experiments were performed under either a N_2 or an Ar atmosphere with degassed solvents.

***trans-fac*-[Ru^{II}(Cl)(bpea)(bpy)](BF$_4$)·1.1CH$_2$Cl$_2$, 2·1.1CH$_2$Cl$_2$.** A 186 mg (0.82 mmol) sample of bpea was dissolved in 10 mL of MeOH and added to a brown solution of 200.0 mg (0.82 mmol) of $RuCl_3 \cdot 2H_2O$ dissolved in 10 mL of MeOH under vigorous magnetic stirring. A brown solid immediately precipitated out of the solution, which was filtered in a Büchner funnel, washed with MeOH and ether, and dried under vacuum. The solid obtained in this manner, 59 mg (1.38 mmol) of LiCl, and 80 mL of 3:1 EtOH/H_2O solution were added under an Ar atmosphere in a round-bottomed 250 mL Schlenck tube under magnetic stirring. Then 0.096 mL (0.69 mmol) of NEt_3 was added and the brown mixture stirred for 20 min at room temperature, upon which it progressively became a dark green solution. At this point 72 mg (0.46 mmol) of 2,2′-bpy dissolved in 2 mL of EtOH was added, and the resulting solution was maintained at reflux for 3.5 h. Upon cooling to room temperature, the volume was reduced at low pressure to 20 mL and the solution filtered on a frit to eliminate small amounts of a dark brown solid. Afterward 2 mL of a saturated aqueous solution of $NaBF_4$ was added to the solution, and the mixture was extracted with CH_2Cl_2. The organic phase was then dried over anhydrous $MgSO_4$ and the sovent removed under reduced pressure. A dark red solid was obtained which was washed with water and ether and dried under vacuum. Yield: 260 mg (42.5%). Anal. Found (Calcd) for $C_{25.5}H_{27.2}BCl_{3.2}F_4N_5Ru$: C, 43.0 (42.9); H, 3.9 (4.2); N, 10.0 (10.0). ^{1}H NMR (d_6-acetone, 500 MHz): δ 1.038 (t, $J_{12-13} = 7.0$ Hz, H13), 2.34 (qua, H12), 4.35 (d, $J_{11i-11o} = 16.5$ Hz, H11o), 4.49 (d, H11i), 7.42 (dd, $J_{7-6} = 6.0$ Hz, $J_{7-8} = 8.0$ Hz, H7), 7.49 (ddd, $J_{4-5} = 5.1$ Hz, $J_{4-3} = 7.9$ Hz, $J_{4-2} = 1.25$ Hz, H4), 7.53 (d, $J_{9-8} = 8.0$ Hz, H9), 7.83 (dt, $J_{8-6} = 1.5$ Hz, H8), 8.02 (dt, $J_{3-2} = 7.9$ Hz, $J_{3-5} = 1.5$ Hz, H3), 8.51 (d, H5), 8.68 (d, H2), 9.61 (d, $J_{6-7} = 6.0$ Hz, H6). ^{13}C NMR (d_6-acetone): 152.6 (C6), 123.79 (C7), 135.77 (C8), 121.13 (C9), 152.3 (C5), 125.79 (C4), 134.71 (C3), 123.26 (C2). For the NMR assignment we have used the same labeling scheme used in the X-ray structure, with H11o being the hydrogen atom from C11 that is directed outside the cavity formed by the bpea ligand upon coordination to the Ru metal center and H11i the one directed toward the inside of the bpea cavity. $E_{1/2} = 0.738$ V.

***trans-fac*-[Ru^{II}(bpea)(bpy)(H$_2$O)](PF$_6$)$_2$, 3.** A 50 mg (0.072 mmol) sample of **2·1.1CH$_2$Cl$_2$** was added to 20 mL of water and the resulting mixture refluxed for 30 min. The orange solution obtained was allowed to reach room temperature and then filtered on a frit. Afterward 2 mL of a saturated aqueous solution of NH_4PF_6 was added, upon which an orange solid precipitated. This solid was washed with cold water and ether and dried under vacuum. Yield: 52 mg (90%). Anal. Found (Calcd) for $C_{24}H_{27}F_{12}N_5OP_2Ru$: C, 36.4 (36.0); H, 3.4 (3.7); N, 8.8 (8.7). ^{1}H NMR (D_2O, 200 MHz): δ 0.86 (t, $J_{12-13} = 8.0$ Hz, H13), 2.13 (qua, H12), 4.15 (d, $J_{11i-11o} = 16.6$ Hz, H11o), 4.27 (d, H11i), 7.42 (m, H7, H4, H9), 7.79 (t, $J_{8-7} = J_{8-9} = 7.4$ Hz, H8), 8.05 (t, $J_{3-4} = J_{3-5} = 8.0$ Hz, H3), 8.54 (m, H5, H2), 8.80 (d, $J_{6-7} = 5.2$ Hz, H6).

[Ru^{II}(bpea)(H$_2$O)$_3$](*p*-*tos*)$_2$, 6. A 50 mg (0.086 mmol) sample of **5·1.5H$_2$O** was dissolved in 5 mL of a 0.1 M solution of CF_3COOD in D_2O previously degassed with Ar. The pink solution was then heated

(2) (a) Lau, T.-C.; Che, C.-M.; Lee, W.-O.; Poon, C.-K. *J. Chem. Soc., Chem. Commun*. **1988**, 1406. (b) Che, C.-M.; Yam, V. W. W.; Mak, T. C. W. *J. Am. Chem. Soc*. **1990**, *112*, 2284. (c) Grover, N.; Ciftan, S. A.; Thorp, H. H. *Inorg. Chim. Acta* **1995**, *240*, 335. (d) Morice, C.; Lemaux, P.; Moinet, C.; Simonneaux, G. *Inorg. Chim. Acta* **1998**, *273*, 142.

(3) (a) Dobson, J. C.; Seok, W. K.; Meyer, T. J. *Inorg. Chem*. **1986**, *25*, 1513. (b) Goldstein, A. S.; Beer, R. H.; Drago, R. S. *J. Am. Chem. Soc*. **1994**, *116*, 2424. (c) Stultz, L. K.; Binstead, R. A.; Reynolds, M. S.; Meyer, T. J. *J. Am. Chem. Soc*. **1995**, *117*, 2520. (d) Cheng, W.-C.; Yu, W.-Y.; Cheung, K.-K.; Peng, S.-M.; Poon, C.-K.; Che, C.-M. *Inorg. Chim. Acta* **1996**, *242*, 105. (e) Ho, C.; Che, C.-M.; Lau, T.-C. *J. Chem. Soc., Dalton Trans*. **1990**, 967. (f) Carmona, D.; Cativiela, C.; Elipe, S.; Lahoz, F. J.; Lamata, M. P.; Pilar, M.; Deviu, L. R.; Oro, L. A.; Vega, C.; Viguri, F. *Chem. Commun*. **1997**, 2351.

(4) (a) Thompson, M. S.; Meyer, T. J. *J. Am. Chem. Soc*. **1982**, *104*, 4106. (b) Roecker, L. E.; Meyer, T. J. *J. Am. Chem. Soc*. **1987**, *109*, 746−754. (c) Marmion, M. E.; Takeuchi, K. J. *J. Am. Chem. Soc*. **1988**, *110*, 1742. (d) Binstead, R. A.; MacGuire, M. E.; Dovletoglou, A.; Seok, W. K.; Roecker, L. E.; Meyer, T. J. *J. Am. Chem. Soc*. **1992**, *114*, 173. (e) Che, C. M.; Ho, C.; Lau, T. C. *J. Chem. Soc., Dalton Trans*. **1991**, 1259. (f) Catalano, V. J.; Heck, R. A.; Immoos, C. E.; Ohman, A.; Hill, M. G. *Inorg. Chem*. **1998**, *37*, 2150.

(5) (a) Moyer, B. A.; Sipe, B. K.; Meyer, T. J. *Inorg. Chem*. **1981**, *20*, 1475−1480. (b) Seok, W. K.; Son, Y. J.; Moon, S. W.; Lee, H. N. *Bull. Korean Chem. Soc*. **1998**, *19*, 1084.

(6) (a) Roecker, L.; Dobson, J. C.; Vining, W. J.; Meyer; T. J. *Inorg. Chem*. **1987**, *26*, 779. (b) Acquaye, J. H.; Muller, J. G.; Takeuchi, K. J. *Inorg. Chem*. **1993**, *32*, 160. (c) Hua, X.; Lappin, A. G. *Inorg. Chem*. **1995**, *34*, 992. (d) Szczepura, L. F.; Maricich, S. M.; See, R. F.; Churchill, M. R.; Takeuchi, K. J. *Inorg. Chem*. **1995**, *34*, 4198. (e) Hua, X.; Shang, M.; Lappin, A. G. *Inorg. Chem*. **1997**, *36*, 3735.

(7) Dovletoglou, A.; Adeyemi, S. A.; Meyer, T. J. *Inorg. Chem*. **1996**, *35*, 4120.

(8) Bessel, C. A.; Margarucci, J. A.; Acquaye, J. H.; Rubino, R. S.; Crandall, J.; Jircitano, A. J.; Takeuchi, K. J. *Inorg. Chem*. **1993**, *32*, 5779.

(9) Pal, S.; Chan, M. K.; Armstrong, W. H. *J. Am. Chem. Soc*. **1992**, *114*, 6398.

(10) (a) Bernhard, P.; Lehmann, H.; Ludi, A. *J. Chem. Soc., Chem. Commun*. **1981**, 1216. (b) Bernhard, P.; Burgi, H.-B.; Hauser, J.; Lehmann, H.; Ludi, A. *Inorg. Chem*. **1982**, *21*, 3936. (c) Bernhard, P.; Biner, M.; Ludi, A. *Polyhedron* **1989**, *8*, 1095.

to reflux, at which point 20 mg of bpea dissolved in 1 mL of 0.1 M CF_3COOD in D_2O was added. This addition was done in 10 consecutive additions of 100 μL portions within 20 min. The flask was then allowed to cool to room temperature and Zn(Hg) thoroughly washed with D_2O added to prevent the appearance of oxidated products. KPF_6 was also added to separate small amounts of $[Ru(bpea)_2]^{2+}$ formed during the reaction as its PF_6 salt. A 50 μL sample of a 40 wt % NaOD solution in D_2O was then added till approximately pH 7, and then the pH was reduced to 1 again upon addition of 39 μL of 99.5% CF_3COOD acid. The evolution of the products formed was monitored by cyclic voltammetry experiments. The compound was characterized in solution (ESI-MS, NMR, UV−vis, and CV) since multiple attempts to isolate it in the solid state have failed. ESI-MS: *m/z* (assignment) 727 ($[Ru^{II}(bpea)(H_2O)_3](p\text{-tos})_2H^+$), 668 ($[Ru^{II}(bpea)(H_2O)_3](p\text{-tos})(CF_3COO)H^+$), 554 ($[Ru^{II}(bpea)(H_2O)_3](p\text{-tos})$). ^{1}H NMR ($D_2O$, 200 MHz): δ 1.42 (t, $J_{13-12} = 6.7$ Hz, H13), 3.40 (qua, $J_{12-13} = 6.7$ Hz, H12), 4.16 (d, $J_{11o-11i} = 16.5$ Hz, H11o), 4.32 (d, H11i), 7.30 (d + t, H7 + H9), 7.65 (t, $J_{8-7} = J_{8-9} = 7.3$ Hz, H8), 8.9 (d, $J_{6-7} = 6.3$ Hz, H6). $E_{1/2} = 0.384$ V.

Instrumentation and Measurements. IR spectra were recorded on a Mattson Satellite FT-IR spectrometer with KBr pellets. UV−vis spectroscopy was performed on a diode array HP-89532A-UV−vis spectrophotometer and a Cary 50 Scan (Varian) UV−vis spectrophotometer with 1 cm quartz cells. pH measurements were done using a Micro-pH-2000 from Crison. Cyclic voltammetric (CV) experiments were performed on a PAR 263A EG&G potentiostat using a three-electrode cell. Glassy carbon disk electrodes (3 mm diameter) from BAS were used as working electrodes, platinum wire as the auxiliary electrode, and SSCE as the reference electrode. All cyclic voltammograms presented in this work were recorded at a 100 mV/s scan rate under a nitrogen atmosphere. The complexes were dissolved in previously degassed solvents containing the necessary amount of supporting electrolyte to yield a 0.1 M ionic strength solution. In acetonitrile (n-Bu_4N)(PF_6) was used as the supporting electrolyte. In aqueous solutions the pH was adjusted from 0 to 2 with HCl. Sodium chloride was added to keep a minimum ionic strength of 0.1 M. From pH 2 to pH 10, 0.1 M phosphate buffers were used, and from pH 10 to pH 12 diluted, CO_2-free, NaOH was used. All $E_{1/2}$ values reported in this work were estimated from cyclic voltammetry as the average of the oxidative and reductive peak potentials ($E_{p,a} + E_{p,c}$)/2. Unless explicitly mentioned, the concentration of the complexes was approximately 1 mM. Bulk electrolysis was carried out using carbon felt from SOFACEL as the working electrode.

^{1}H NMR spectroscopy was performed on a Bruker DPX 200 MHz or a Bruker 400 MHz spectrometer. Samples were run in acetone-d_6 or deuterium oxide with internal references (residual protons and/or tetramethylsilane). Elemental analyses were performed using a CHNS−O elemental analyzer, EA-1108, from Fisons. For gas chromatography a GC-17A gas chromatograph from Shimadzu was used. The ESI-MS experiments were performed on a Navigator LC/MS chromatograph from Thermo Quest Finigan, using MeOH/H_2O as the mobile phase.

Chemical catalysis was performed using the following general conditions: 1.0 mM catalyst/100 mM substrate/200 mM Ce(IV)/H_2O−acetone (1:1). Electrocatalytic studies at neutral pH were performed in a phosphate buffer solution, at an applied potential of 0.9 V vs SSCE. A carbon felt electrode from SOFACEL was used as the working electrode. In basic media a 0.2 M NaOH solution was used, and the potential applied was 0.6 V vs SSCE. The ratio catalyst:substrate was 1:100 in both cases. Benzyl alcohol and benzaldehyde evolution was followed on a Shimadzu GC-17A gas chromatography apparatus, after extraction from the reaction mixture with an ethereal solution of naphthalene, used as an internal standard.

X-ray Structure Determination. Suitable crystals of *trans-fac*-[Ru(bpea)(bpy)(H_2O)](PF_6)$_2$, **3**, were grown from water as thin red rods. Intensity data were collected at 223 K on a Stoe image plate diffraction system using Mo Kα graphite-monochromated radiation. The parameters were image plate distance 70 mm, ϕ scans 0−192°, step $\Delta\phi$ = 1°, 2θ range 3.27−52.1°, $d_{max}-d_{min}$ = 12.45−0.81 Å. The structure was solved by direct methods using the program SIR-97.[11a] The refinement and all further calculations were carried out using SHELXL-97.[11b] The H atoms were located from difference Fourier maps and refined isotropically. The non-H atoms were refined anisotropically using weighted full-matrix least-squares on F^2. The cation possesses C_s symmetry, with the mirror plane bisecting the two ligands. Atoms Ru, O1, N2, C12, and C13 all lie in the mirror plane. The bond lengths and angles are normal within experimental error.

Scheme 1. Synthetic Strategy

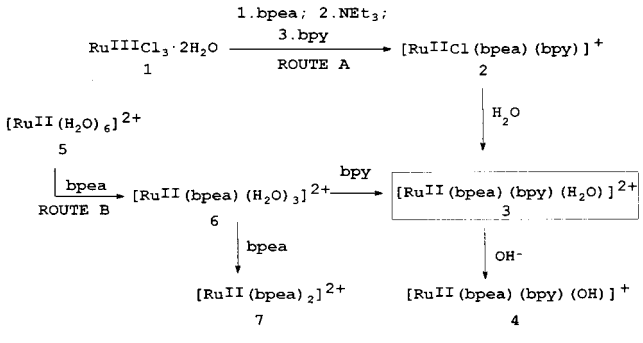

Results and Discussion

Synthesis, Structure, and Stereoisomeric Analysis. The synthetic strategy followed for the preparation of the complexes is outlined in Scheme 1. Two different routes have been used to prepare the Ru−aqua complex **3**. Route A is the classical route involving the formation of a bpea−Ru(III) complex, which is then reduced with NEt_3 in the presence of bpy. Finally the remaining Cl ligand is simply substituted by gently refluxing **2** in water for 30 min. No silver salts are needed in this case. The Ru−aqua complex **3** can also be prepared using $[Ru^{II}(H_2O)_6]^{2+}$, **5**, as the starting material following route B. The addition of bpea to a solution of **5** produces a yellow solution of the $[Ru^{II}(bpea)(H_2O)_3]^{2+}$ complex, **6**. All attempts to isolate **6** in the solid state have failed due to the high instability of the formed complex.

In acidic solution, at pH 1, the reaction of $[Ru^{II}(H_2O)_6]^{2+}$, **5**, and bpea produces the trisaqua complex **6** ($E_{1/2} = 0.384$ V, $\Delta E = 124$ mV) together with an intermediate ($E_{1/2} = 0.171$ V, $\Delta E = 134$ mV) (cyclic voltammogram shown in the Supporting Information) and small amounts of $[Ru^{II}(bpea)_2]^{2+}$, **7**. The latter can be precipitated from the solution by adding KPF_6 while the rest of the products remain in solution. The intermediate can be tentatively assigned to $[Ru^{II}(Hbpea)(H_2O)_4]^{3+}$ where bpea

$$[Ru^{II}(Hbpea)(H_2O)_4]^{3+} \rightarrow [Ru^{II}(bpea)(H_2O)_3]^{2+} + H_3O^+ \quad (3)$$

acts as a didentate ligand and only two water molecules have been substituted from the initial Ru−hexakisaqua complex. This intermediate progressively transforms into the trisaqua complex as the reaction proceeds (see eq 3). The assignment is made on the basis of reactivity patterns, spectral properties, and electrochemical considerations (vide infra). It seems logical to assume that the substitution of the aqua ligands in **6** takes place in a stepwise manner given the labile nature of the aqua ligands in the Ru−aqua complexes with regard to their substitution by polypyridylic ligands. Thus, several complexes with different degrees of substitution can potentially be obtained. In particular, the addition of excess bpea ligand drives the reaction toward the formation of $[Ru^{II}(bpea)_2]^{2+}$, **7** ($E_{1/2} = 0.893$ V, $\Delta E = 94$ mV))[14d] as the only product, and the addition of bpy generates $[Ru^{II}(bpea)(bpy)(H_2O)]^{2+}$, **3**, also as the only product observed

(11) (a) Cascarano; et al. SIR-97. *Acta Crystallogr*. **1996**, *A52*, C79. (b) G. M. Sheldrick, SHELXL-97, Universität Göttingen, Göttingen, Germany, 1999.

Table 1. Crystal Data for the Complex $[Ru(bpea)(bpy)(H_2O)](PF_6)_2$ (**3**)

empirical formula	$C_{24}H_{26}N_5ORuP_2F_{12}$	no. of formula units/cell	2
fw	791.51	temp, K	223(2)
cryst syst, space group	monoclinic, $P2_1/m$	λ(Mo Kα), Å	0.71073
a, Å	7.9298(6)	ρ_{calcd}, g/cm^3	1.804
b, Å	18.0226(19)	μ, mm^{-1}	0.755
c, Å	10.6911(8)	R[a]	0.0261
β, deg	107.549(8)	R_w[a]	0.0611
V, Å^3	1456.8(2)		

[a] $R = [\sum(||F_o| - |F_c||)/\sum|F_o|]$; $R_w = \{[\sum(w(F_o^2 - F_c^2)^2)/\sum(wF_o^4)]^{1/2}\}$.

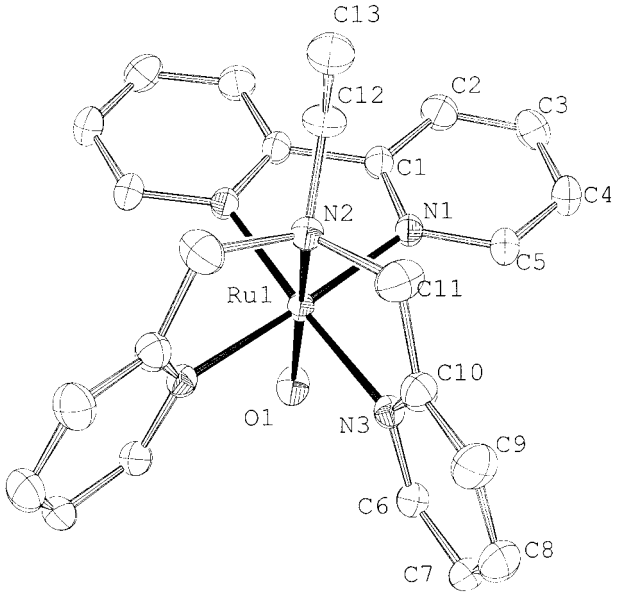

Figure 1. An ORTEP view (thermal ellipsoids are plotted at 50% probability) of the molecular structure of $[Ru^{II}(bpea)(bpy)H_2O]^{2+}$ cation including the atom numbering scheme.

(see Scheme 1). Furthermore, cyclic voltammetric experiments show that an enhancement of the solution basicity up to pH 7 followed by a reduction again to pH 1 drives the reaction stated in eq 3 toward the formation solely of the trisaqua complex. This process is induced by the deprotonation of the partially coordinated bpea ligand in the intermediate complex and by the decrease of the $[H_3O^+]$ upon increasing the pH.

Crystallographic data for complex **3** are presented in Table 1 whereas Figure 1 shows the cationic moiety of complex **3.** Further crystallographic data including a vision of the crystal packing through the X axis (cell with $X = 5$, $Y = 1$, $Z = 1$) can be seen in the Supporting Information. In complex **3** the tripodal bpea ligand is coordinated in a facial fashion and the N atoms of the bpy ligands occupy the positions trans to the N atoms of the pyridyl groups of the bpea ligand. Finally the oxygen atom of the water molecule is situated trans to the aliphatic N atom of bpea.

There is a mirror plane that bisects the molecule and contains the Ru, O1, N2 (aliphatic N from bpea), and C12 and C13 (ethyl group bonded to the aliphatic nitrogen from bpea) atoms. All bond distances and angles are comparable to those of similar complexes that have already been described in the literature.[12,14d] The bond angles deviate from those of the ideal octahedron due to the steric constraints imposed by the tridentate and didentate ligands. Thus, angles below 90° are obtained for *cis*-NRuN with N atoms belonging to the same ligand (either bpea or bpy), and bond angles above 90° are found for *cis*-NRuN with N atoms belonging to different ligands. The Ru−O bond is slightly bent

Chart 1. Possible Diastereoisomers

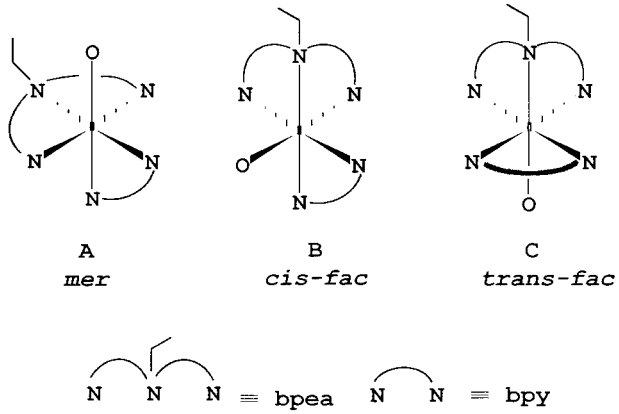

toward the bpy ligand, and as a consequence the NRuO angles for the bpy ligand are 2.12° below 90° whereas the *cis*-NRuO angles for the bpea ligand are 3.71° above 90°.

All six F atoms of the PF_6^- anions interact with the $[Ru(bpea)(bpy)(H_2O)]^{2+}$ cation through extensive hydrogen bonding, forming a 3D network over the crystal. The cations are piled up, forming four pseudochains within the unit cell along the X direction; those pseudochains have the same direction in the Z axis, but they have opposite directions in the Y axis (see the Supporting Information).

A list of the most significant hydrogen-bonding distances and angles can be found in the Supporting Information. The hydrogen atoms of the aqua ligand present relatively strong hydrogen bonding with F1 and F6. Furthermore, all F atoms of the PF_6^- counteranions display weak to moderate hydrogen bonding with hydrogen atoms of both the bpea and bpy ligands. A detailed analysis of the hydrogen bonding indicates that each PF_6^- anion interacts primarily with three cationic molecules at a relatively similar YZ level and to a lesser extent with three more cations from the lower contiguous YZ layer.

The bpea ligand is a flexible molecule that can act in both meridional[13] and facial[14] fashions when coordinated to a transition metal. Chart 1 shows the three possible diastereoisomers that could be potentially obtained with the bpea, bpy, and aqua ligands coordinating a metal center in an octahedral manner.

X-ray diffraction analysis shows that, in the solid state for complex **3**, the bpea ligand is facially coordinated (see Figure 1) with the aqua ligand trans to the aliphatic bpea N atom (isomer C, trans-fac; Chart 1). NMR spectra of complex **3**, vide infra, reveal that in solution the facial coordination is still kept since a meridional arrangement as in case A (mer) would leave the pyridyl bpy rings magnetically nonequivalent. Moreover, from NMR spectra one can also conclude that isomer B (cis-fac) is not present either since for this isomer all pyridylic rings, from bpea and bpy ligands, would become magnetically nonequivalent.

(12) (a) Llobet, A.; Hodgson, D. J.; Meyer, T. J. *Inorg. Chem.* **1990**, *29*, 3760. (b) Gilbert, J. A.; Eggleston, D. S.; Murphy, W. R.; Geselowitz, D. A.; Gerstern, S. W.; Hodgson, D. J.; Meyer, T. J. *J. Am. Chem. Soc.* **1985**, *107*, 3785.

(13) Pal, S.; Olmstead, M. M.; Armstrong, W. H. *Inorg. Chem.* **1995**, *34*, 4708.

(14) (a) Das, B. K.; Chakravarty, A. R. *Inorg. Chem.* **1990**, *29*, 2078. (b) Das, B. K.; Chakravarty, A. R. *Inorg. Chem.* **1991**, *30*, 4978. (c) Sudha, C.; Mandal, S. K.; Chakravarty, A. R. *Inorg. Chem.* **1998**, *37*, 270. (d) Romero, I.; Rodríguez, M.; Llobet, A.; Collomb-Dunand-Sauthier, M.-N.; Deronzier, A.; Parella, T.; Soteckli-Evans, H. *J. Chem. Soc., Dalton Trans.* **2000**, 1689.

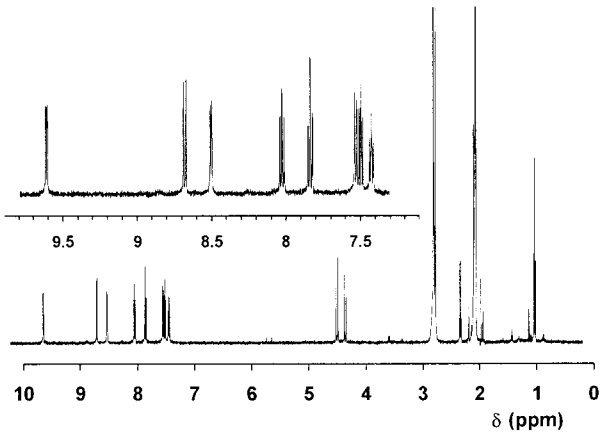

Figure 2. ^{1}H NMR spectra of the complex $[Ru^{II}(Cl)(bpea)(bpy)]^+$, **2,** registered in d_6-acetone.

Therefore, X-ray analysis and solution NMR experiments are consistent with the presence of only the trans-fac isomer both in the solid state and in solution.

Spectroscopic Properties. The ^{1}H NMR spectra of the complexes described in this work were recorded in acetone-d_6 or deuterium oxide and are assigned in the Experimental Section. Figure 2 shows the ^{1}H NMR spectrum of **3**; the corresponding COSY and NOESY 2D NMR spectra and all the spectra for complex **2** are presented as Supporting Information. All resonances in Figure 2 can be unambiguously assigned taking into account the symmetry of the molecule and the integrals and with the aid of the 2D NMR spectra.

The ^{1}H NMR spectrum of **2** in the 7.2−9.7 ppm zone clearly shows eight separate resonances, revealing the presence of only two distinct pyridyl rings, being consistent only with isomer C in Chart 1.

Upon coordinating to the Ru metal center the benzylic hydrogen atoms (H11i, H11o) become magnetically different. H11i is the benzylic hydrogen atom directed into the bpea cavity, whereas H11o is the one headed toward the bpy ligand. The 2D NOESY map together with the crystal structure allows each one to be fully identified since H11i presents a very weak interligand NOE effect with H5 (d = 4.275 Å) and a strong one with H11o (d = 2.842 Å). The opposite is observed for H9 ($d_{H11i-H9}$ = 2.496 Å, $d_{H11o-H9}$ = 3.108 Å). The benzylic hydrogens also display NOE effects with the hydrogen atoms of the bpea ethyl group.

UV−vis spectral features for the bpea and bpy ligands and for complexes **2, 3, 4, 6,** and **7** described in the present work are summarized in Table 2. For the ligands, only $\pi-\pi^*$ bands are observed above 240 nm.

Complexes $[Ru^{II}(bpea)(H_2O)_3]^{2+}$, **6**, and $[Ru^{II}(bpea)_2]^{2+}$, **7**, also present these ligand-based $\pi-\pi^*$ bands at relatively similar energies and an intense and broad d$\pi-\pi^*$ band at 410 and 380 nm, respectively, due to a series of MLCT transitions and their vibronic components. The aqua, hydroxo, and chloro complexes $[Ru^{II}(bpea)(bpy)(X)]^{n+}$ (X = H_2O, n = 2; X = OH or Cl, n = 1) display two ligand-based $\pi-\pi^*$ bands below 300 nm. Above 300 nm the aqua complex **3** shows two bands at 360 and 468 nm that can be tentatively assigned to d$\pi-\pi^*$ bpea and bpy transitions, respectively, by comparison with our data and previous data reported in the literature.[14d,15] For the hydroxo complex **4**, the two MLCT bands are shifted to longer wavelengths with regard to the corresponding Ru−aqua complex **3**, due to the relative destabilization of dπ(Ru) levels provoked by the hydroxo ligand.[16] A similar band shifting is also observed for the chloro complex **2**.

A pK_a of 11.07 can be calculated from acid−base spectrophotometric titration of **3** (presented as Supporting Information), giving eight isosbestic points (492, 434, 368, 304, 294, 268, 248, and 236 nm).

$$[Ru^{II}(bpea)(bpy)(H_2O)]^{2+} \rightarrow [Ru^{II}(bpea)(bpy)(OH)]^{+} + H^{+} \quad (4)$$

$$pK_a(Ru^{II}-OH_2) = 11.07$$

Figure 3 presents the UV−vis spectra of complex **3** at pH 1 and the in situ generated $[Ru^{III}(bpea)(bpy)(H_2O)]^{3+}$ and $[Ru^{IV}(bpea)(bpy)(O)]^{2+}$ using Ce(IV) as the oxidant. The redox titration corresponding to the oxidation of Ru(II) to Ru(III) performed under these conditions exhibits five isosbestic points (320, 298, 278, 252, and 242 nm) which are amplified in the inset in the 220−350 nm region. The oxidation of Ru(III) to Ru(IV) also displays isosbestic points at 342, 318, 310, and 264 nm, and the spectra are shown as Supporting Information. The chemically generated $[Ru^{IV}(bpea)(bpy)(O)]^{2+}$ complex is featureless in the 300−800 nm region in accordance with other related Ru^{IV}=O complexes reported in the literature.[16,17]

Redox Chemistry and Catalytic Properties. Figure 4 displays the Pourbaix diagram of complex **3** based on the $E_{1/2}$ vs pH values obtained from cyclic voltammetry experiments (representative CV experiments are presented as Supporting Information). The pH dependency of the redox potentials in complex **3** is due to the aqua ligand bonded to the ruthenium metal center (vide supra) that deprotonates in basic media (p$K_a(Ru^{II}-OH_2)$ = 11.07) to form the corresponding hydroxo species $Ru^{II}-OH$. At pH 1.4 in a 0.05 M $HClO_4$ solution, only one chemically and electrochemically reversible wave is observed at $E_{1/2}$ = 0.655 V, which is due to the Ru(III)/Ru(II) couple ($E_{p,a}$ = 0.694 V, $E_{p,c}$ = 0.616 V, $\Delta E = E_{p,a} - E_{p,c}$ = 0.078 V).

$$[Ru^{III}(bpea)(bpy)(OH)]^{2+} + 1e^{-} + 1H^{+} \rightarrow [Ru^{II}(bpea)(bpy)(H_2O)]^{2+} \quad (5)$$

At basic pH two redox processes can be detected. For instance at pH 10.9 two chemically reversible redox waves at $E_{1/2}$ = 0.130 V and $E_{1/2}$ = 0.287 V are observed. The first wave is also electrochemically reversible and is assigned to the Ru(III)/Ru(II) couple ($E_{p,a}$ = 0.166 V, $E_{p,c}$ = 0.094 V, $\Delta E = E_{p,a} - E_{p,c}$ = 0.072 V). The second wave has lower intensity and is due to the Ru(IV)/Ru(III) couple ($E_{p,a}$ = 0.382 V, $E_{p,c}$ = 0.212 V, $\Delta E = E_{p,a} - E_{p,c}$ = 0.170 V). For this type of complex it is

$$[Ru^{IV}(bpea)(bpy)(O)]^{2+} + 1e^{-} + 1H^{+} \rightarrow [Ru^{III}(bpea)(bpy)(H_2O)]^{2+} \quad (6)$$

generally accepted that the lower intensity of this wave with regard to the corresponding Ru(III)/Ru(II) is due to slow

(15) (a) Drago, R. S. *Physical Methods in Chemistry*; W. B. Saunders Co.: Philadelphia, London, Toronto, 1977. (b) Meyer, T. J. *Pure Appl. Chem*. **1986**, *58*, 1193. (c) Barqawi, K.; Llobet, A.; Meyer, T. J. *J. Am. Chem. Soc*. **1988**, *110*, 7751.

(16) Takeuchi, K. J.; Thompson, M. S.; Pipes, D. W.; Meyer, T. J. *Inorg. Chem*. **1984**, *23*, 1845.

(17) (a) Dobson, J. C.; Meyer, T. J. *Inorg. Chem*. **1988**, *27*, 3283. (b) Llobet, A.; Doppelt, P.; Meyer, T. J. *Inorg. Chem*. **1988**, *27*, 514. (c) Cheng, W. C.; Yu, W. Y.; Cheung, K. K.; Che, C. M. *J. Chem. Soc., Dalton Trans*. **1994**, 57.

Table 2. UV−Vis Spectral Data for the bpea and bpy Ligands and for Complexes **2**, **3**, **4**, and **6**

compound	solvent	λ_{max} (nm)	ϵ (M^{-1} cm^{-1})	assignment
bpea	0.1 M HCl (H_2O)	258	10274	$\pi-\pi^*$
bpy	0.1 M HCl (H_2O)	239	7660	$\pi-\pi^*$
		300	15566	$\pi-\pi^*$
$[Ru(bpea)(H_2O)_3]^{2+}$	0.1 M CF_3CO_2D (H_2O)	250	14238	$\pi-\pi^*$
		410	4911	$d\pi-\pi^*$
$[Ru(bpea)_2](PF_6)_2$	CH_3CN	250	18057	$\pi-\pi^*$
		380	14472	$d\pi-\pi^*$
		566	167	d−d
$[Ru(bpea)(bpy)(\mathbf{H_2O})](PF_6)_2$	pH 5.82 (H_2O)	246	18755	$\pi-\pi^*$
		292	31430	$\pi-\pi^*$
		360	12257	$d\pi-\pi^*$ (bpea)
		468	96048	$d\pi-\pi^*$ (bpy)
$[Ru(bpea)(bpy)(\mathbf{OH})](PF_6)$	pH 12.94 (H_2O)	248	19162	$\pi-\pi^*$
		296	28510	$\pi-\pi^*$
		384	12786	$d\pi-\pi^*$ (bpea)
		514	5428	$d\pi-\pi^*$ (bpy)
$[Ru(\mathbf{Cl})(bpea)(bpy)](PF_6)$	CH_3CN	248	17219	$\pi-\pi^*$
		296	29617	$\pi-\pi^*$
		380	13108	$d\pi-\pi^*$ (bpea)
		504	5915	$d\pi-\pi^*$ (bpy)

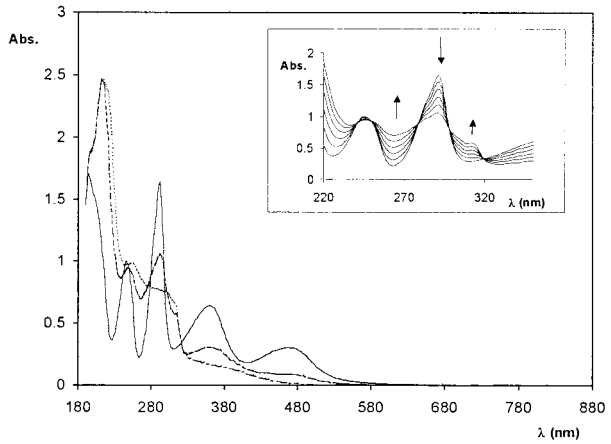

Figure 3. UV−vis absorption spectra at pH 1.3 of **3** (—) and of chemically generated $[Ru^{III}(bpea)(bpy)(OH)]^{2+}$ (•••) and $[Ru^{IV}(bpea)(bpy)(O)]^{2+}$ (---) by addition of stoichiometric amounts of Ce(IV). The inset shows the redox spectrophotometric titration performed by sequential addition of 100 μL of 50 mM Ce(IV) to the original solution to reach $[Ru^{III}(bpea)(bpy)(H_2O)]^{3+}$.

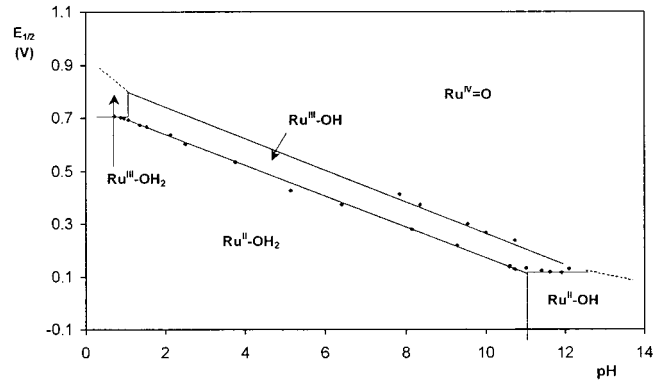

Figure 4. $E_{1/2}$ vs pH or the Pourbaix diagram of **3**. The pH/potential regions of stability for the various oxidation states and their dominant proton compositions are indicated by using abbreviations such as Ru^{II}-OH_2, for example, for $[Ru^{II}(bpea)(bpy)(H_2O)]^{2+}$. The p$K_a$ values are shown by the vertical solid lines in the various E/pH regions.

heterogeneous electron-transfer kinetics from the solution to the electrode surface.[17a,18] At lower pH the second oxidation of Ru(III) to Ru(IV) is not observed at all, and it is also believed to be due to the same phenomenon.

(18) (a) Cabaniss, G. E.; Diamantis, A. A.; Murphy, W. R.; Linton, R. W.; Meyer, T. J. *J. Am. Chem. Soc*. **1985**, *107*, 1846. (b) Catalano, V. J.; Kurtaran, R.; Heck, R. A.; Ohman, A.; Hill, M. G. *Inorg. Chim. Acta* **1999**, *286*, 181.

Table 3. Electrochemical Data at pH 7 in μ = 0, 1 M Phosphate Buffer Solutions and pK_a for Related Ru−Aqua Complexes

	$E_{1/2}$ (V)						
complex[a]	IV/III	III/II	IV/II	$\Delta E_{1/2}$[b]	p$K_{a,II}$[c]	p$K_{a,III}$[c]	ref
$[Ru(trpy)(acac)(OH_2)]^{2+}$	0.56	0.19	0.38	370	11.2	5.2	25
$[Ru(bpea)(bpy)(OH_2)]^{2+}$	0.46	0.34	0.40	120	11.1	1.2	*d*
$[Ru(trpy)(tmen)(OH_2)]^{2+}$	0.59	0.36	0.48	230	10.8	0.9	25
$[Ru(bpy)_2(py)(OH_2)]^{2+}$	0.53	0.42	0.48	110	10.8	0.9	25
$[Ru(trpy)(bpy)(OH_2)]^{2+}$	0.62	0.49	0.56	130	9.7	1.7	25
$[Ru(bpy)_2(PPh_3)(OH_2)]^{2+}$	0.76	0.50	0.63	260	−	−	25
$[Ru(trpy)(dppene)(OH_2)]^{2+}$	1.53	1.17	1.35	360	−	−	25

[a] Ligand abbreviations used: acac = acetylacetonate; tmen = *N*,*N*,*N*′,*N*′-tetramethylethylenediamine; dppene = *cis*-1,2-bis(diphenylphosphino)ethylene. [b] $\Delta E_{1/2} = E_{1/2}(IV/III) - E_{1/2}(III/II)$ in millivolts. [c] p$K_{a,II}$ and p$K_{a,III}$ represent the pK_a of the corresponding $Ru^{II}-OH_2$ and $Ru^{III}-OH_2$ species, respectively. [d] This work.

Finally at pH 12.6 only one chemically irreversible redox couple is observed at $E_{p,a}$ = 0.242 V, with nearly double intensity with regard to the previous ones, that is assigned to the Ru(IV)/Ru(II) couple. Increasing the scan rate from 100 to 300 mV provokes the appearance of a small returning wave.

$$[Ru^{IV}(bpea)(bpy)(O)]^{2+} + 2e^- + H^+ \rightarrow [Ru^{II}(bpea)(bpy)(OH)]^+ \quad (7)$$

The Pourbaix diagram shown in Figure 4 offers a complete thermodynamic picture of the different species derived from the $Ru^{II}-OH_2$ complex **3**, as a function of proton and/or electron gains or losses. In the diagram are labeled the different E/pH zones of stability for the different species related to **3**. The pK_a for the $Ru^{III}-OH_2$ and $Ru^{II}-OH_2$ species can be calculated for instance from the slope brakes of the Ru^{III}/Ru^{II} couple.

$$[Ru^{III}(bpea)(bpy)(H_2O)]^{3+} \rightarrow [Ru^{III}(bpea)(bpy)(HO)]^{2+} + H^+ \quad (8)$$

$$pK_a(Ru^{III}-OH_2) = 1.2$$

For $Ru^{II}-OH_2$ the pK_a value obtained electrochemically coincides with that obtained spectrophotometrically.

Table 3 presents pK_a and electrochemical data for complex **3** and related polypyridylruthenium−aqua complexes for purposes of comparison. As can be observed the redox potential for the Ru(IV)/(III) and Ru(III)/(II) couples can be varied by nearly 1 V depending on the ancillary ligands attached to the Ru metal atom. Using $[Ru(trpy)(bpy)(H_2O)]^{2+}$ as a reference, it can be seen that replacing the bpy ligand by the strong σ

donor ligand $acac^-$ (acetylacetonato anionic ligand) strongly influences the III/II redox potential (it decreases by 300 mV) while the IV/III redox potential is affected to a lesser extend (it decreases by 60 mV). This phenomenon is attributed to the fact that σ electron donor ligands produce a stabilization of Ru(III)[7] and necessarily of Ru(IV) since otherwise the IV/III redox potential would be much higher. On the other hand, the opposite effect is observed with ligands that are good π electron acceptors; dppene increases the IV/III redox potential by 910 mV and the III/II redox potential by 680 mV. The latter phenomenon is attributed to the stabilization of Ru(II) by $d\pi-\pi^*$ back-bonding with ligands that have low-lying acceptor levels[7] and also to a destabilization of Ru(IV). The replacement of the trpy ligand by bpea involves the two phenomena just described, and the net effect observed is a balance between them. The bpea ligand is a better σ donor than trpy and therefore should stabilize Ru(III) and Ru(IV). The fact that ΔE(IV/III−III/II) decreases instead of increases as in the $acac^-$ case reveals that a significant π effect is also present in this case. Therefore, the replacement of trpy by bpea produces a notable decrease of π-back-bonding, which is manifested in a destabilization of Ru(II) and a stabilization of Ru(IV). The final balance of σ and π effects produces a ΔE of 120 mV, 10 mV less than in the $[Ru(trpy)(bpy)(H_2O)]^{2+}$ case.

The oxidative properties of $[Ru^{IV}(bpea)(bpy)(O)]^{2+}$ were examined using benzyl alcohol as a probe substrate. It was found that the system "1.0 mM **3**/100 mM $PhCH_2OH$/200 mM Ce(IV)/water−acetone (1:1)" yielded 35 mM benzaldehyde as the only product detected after 2 h of reaction time. A blank experiment in the absence of the Ru catalyst under similar experimental conditions yielded 5 mM benzaldehyde. This implies that this system produces at least 30 redox cycles with a turnover frequency of 0.5 cycle/min.

The oxidation of benzyl alcohol was also performed using the potentiostat as an electron sink, and the experimental results obtained at pH 6.8 and 13.3 are displayed in the Supporting Information. At neutral pH, the system produces again benzaldehyde selectively although now the reaction is much slower. After 10 h, the system "0.5 mM **3**/50 mM $PhCH_2OH$/pH 6.8 phosphate" at an E_{app} of 0.9 V yields 18 mM benzaldehyde, which implies the production of 36 redox cycles with a current efficiency of 82%. Under basic conditions the stability of the catalyst is significantly enhanced, displaying a remarkable activity completely depleting the initial substrate; the system "1 mM **3**/100 mM $PhCH_2OH$/0.2 mM NaOH" at an E_{app} of 0.6 V yielded 30 mM benzaldehyde in 6.5 h with a current efficiency of 44%. At this point benzaldehyde starts being a competitive substrate vis-à-vis of benzyl alcohol and is oxidized to benzoic acid. At 14 h of reaction time there is no alcohol left and the final products are a mixture of benzoic acid and benzaldehyde. Second-order rate constants for the oxidation of benzyl alcohol in the three conditions presented here are estimated to be 0.22 $M^{-1}\,s^{-1}$ (acetone−H_2O (1:1), Ce(IV)), 0.14 $M^{-1}\,s^{-1}$ (pH 6.8, E_{app} = 0.9 V), and 0.015 $M^{-1}\,s^{-1}$ (0.2 M NaOH, E_{app} = 0.9 V). Recently reported second-order rate constants for the oxidation of benzyl alcohol by related Ru=O-type complexes[4f,19] range from 2.4 to 22.0 $M^{-1}\,s^{-1}$. Although the ones reported in the present paper are 1−2 orders of magnitude smaller, they are not strictly comparable since the experimental conditions used are significantly different.

Blank experiments in all the electrocatalytic cases described above were performed under similar conditions but without the Ru catalyst, yielding only trace amounts of benzaldehyde.

The fate of the catalyst is a subject of current investigation. For the electrocatalytic runs at neutral pH a small amount of a ruthenium-containing pink solid is obtained at the end of the experiment. We do not know yet the precise nature of this catalytically inactive solid, but it might be due to either an intermolecular catalyst interaction or the formation of an inactive Ru complex with the final oxidative products coordinated to the metal center. We are currently directing our efforts toward the design and performance of experiments headed to unravel its nature.

In conclusion, the synthesis and characterization of a new family of Ru−bpea complexes is described based on $RuCl_3$ and $Ru(H_2O)_6^{2+}$ as starting materials. The latter generates $Ru-OH_2$ synthetic intermediates that are characterized in solution. A thorough investigation of the redox properties of the monoaqua−Ru complex, $[Ru^{II}(bpea)(bpy)(H_2O)]^{2+}$, allows the σ and π effects exerted by the bpea ligand to the Ru center to be interpreted. Finally the $[Ru^{IV}(bpea)(bpy)(O)]^{2+}$ complex, obtained from the oxidation of the corresponding Ru−aqua complex, displays an outstanding catalytic activity with regard to the oxidation of benzyl alcohol.

Acknowledgment. This research has been financed by MICYT of Spain through Project BQP2000-0458 and with the aid of Grant SGR99/166 from CIRIT Generalitat de Catalunya (Spain), both awarded to A.L. A.L. also thanks Johnson and Matthey for a $RuCl_3 \cdot xH_2O$ loan. I.R. and M.R. are grateful for the award of a postdoctoral grant and a doctoral grant, respectively, from CIRIT. Prof. A. Roglans and Mrs. A. Costa from the University of Girona are gratefully acknowledged for registering the ESI-MS spectra.

Supporting Information Available: Crystallographic information in CIF format for complex **3** together with tables and figures containing synthetic, crystallographic, spectroscopic (UV−vis, 2D NMR), and redox properties. This material is available free of charge via the Internet at http://pubs.acs.org.

IC010064Q

(19) Lebeau, E. L.; Meyer, T. J. *Inorg. Chem.* **1999**, *38*, 2174.